Reinforced Concrete Membrane Elements with Perforations

By F. J. Vecchio[1] and C. C. L. Chan[2]

Abstract: An experimental investigation is described in which perforated reinforced concrete panel elements were subjected to uniformly distributed, monotonically increasing edge loads. Test parameters included the presence of a perforation, detailing of the reinforcement, and type of load condition. It was found that the stress disturbances created by a perforation resulted in significant reductions in element strength and stiffness and localized damage near the opening. The addition of extra reinforcement around the opening partially alleviated this influence. Predictions of panel response were made from nonlinear finite element analyses, using a formulation based on the modified compression field theory. Good accuracy was obtained in the predicted crack patterns, load-deformation responses, reinforcement stresses, ultimate loads, and failure modes. The results suggest that behavior models based on a smeared, rotating crack can adequately represent response under locally complex stress conditions, provided proper consideration is given to concrete compression strain-softening effects and tension-stiffening effects.

Introduction

The modified compression field theory (MCFT) was proposed several years ago as a simple theoretical model for predicting the response of reinforced concrete membrane elements subjected to in-plane forces (Vecchio and Collins 1986). The theory was based on the smeared rotating crack concept with equilibrium, compatibility, and stress-strain relations formulated in terms of average strains and average stresses. New constitutive relations were developed for cracked concrete, reflecting significant influences from compression strain-softening and tension-stiffening effects. Subsequently, the formulations of the MCFT were incorporated into a nonlinear finite element program (Vecchio 1989, 1990).

The constitutive relations of the MCFT were based on the results of an experimental program in which homogeneous, orthotropically reinforced concrete panels were subjected to uniformly distributed edge loads. Thus, the stress and strain conditions within the panels were uniform at all locations. The analytical procedures developed were shown to predict response, under such conditions, extremely well (Vecchio 1989). However, in further verifying the accuracy and applicability of MCFT-based formulations, it is necessary to extend consideration to situations in which nonuniform, rapidly changing, or locally concentrated stress conditions exist. Such conditions may result from discontinuities in geometry, changes in reinforcement details, or concentrated load conditions.

In practical applications, the need to consider stress disturbances in mem-

[1]Assoc. Prof., Dept. of Civ. Engrg., Univ. of Toronto, Toronto, Canada M5S 1A4.

[2]Struct. Engr., M. S. Yolles and Partners, Consulting Engrs., 163 Queen St. E, Suite 200, Toronto, Canada M5A 1S1.

Note. Discussion open until February 1, 1991. To extend the closing date one month, a written request must be filed with the ASCE Manager of Journals. The manuscript for this paper was submitted for review and possible publication on August 2, 1989. This paper is part of the ***Journal of Structural Engineering***, Vol. 116, No. 9, September, 1990. ©ASCE, ISSN 0733-9445/90/0009-2344/$1.00 + $.15 per page. Paper No. 25032.

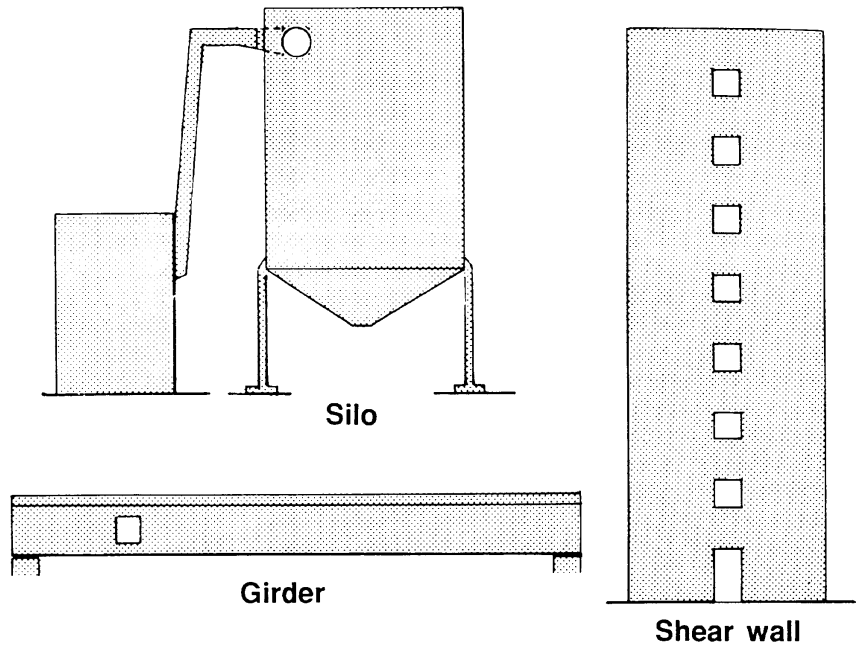

FIG. 1. Examples of Perforated Elements in Reinforced Concrete Membrane Structures

brane elements often arises when the elements contain perforations or cutouts (e.g., see Fig. 1). Various analytical and design procedures have been proposed to ensure satisfactory structural performance under such conditions. Design recommendations typically call for additional reinforcement to be provided around the opening (ACI 1983; Mansur et al. 1985). Analytical approaches are tending to be oriented toward finite element analyses (Haydl 1987; Pool and Lopes 1986; Sato et al. 1987).

This paper describes the results of a limited study made into the behavior of perforated reinforced concrete membranes. The objectives were threefold: (1) To experimentally observe the influence of perforations on element response; (2) to provide data for calibrating analytical procedures; and (3) to test the ability of MCFT-based formulations in accurately predicting response under more complex conditions.

Test Program

The experimental program undertaken consisted of three series of tests involving reinforced concrete panel specimens subjected to in-plane loads. Within each series, three types of panels were fabricated and tested. The panel types differed in respect to the inclusion of an opening and to the detailing of the reinforcement. The primary variable between series of tests was the loading condition imposed, ranging from pure shear to combined shear and biaxial compression, and combined shear and biaxial tension. Table 1 summarizes the specimen parameters and loading conditions for the panels tested. Note that one specimen, panel PC1, failed prematurely, and that the test condition was repeated with panel PC1A.

The test specimens were 890 by 890 by 70-mm concrete panels with orthogonal reinforcement. In those panels for which an opening was specified, a 150-mm square perforation was cast at the center. In all panels, the re-

TABLE 1. Specimen Parameters

Panel number (1)	Panel type (2)	Reinforcement ρ_x (3)	Reinforcement ρ_y (4)	Opening (mm × mm) (5)	Added reinforcement (6)	Loading $v:f_x:f_y$ (7)
			(*a*) Series I			
PC1	Type I	0.0165	0.00825	—	—	1:0:0
PC1A	Type I	0.0165	0.00825	—	—	1:0:0
PC2	Type II	0.0165	0.00825	150 × 150	No	1:0:0
PC3	Type III	0.0165	0.00825	150 × 150	Yes	1:0:0
			(*b*) Series II			
PC4	Type I	0.0165	0.00825	—	—	1:−0.39:−0.39
PC5	Type II	0.0165	0.00825	150 × 150	No	1:−0.39:−0.39
PC6	Type III	0.0165	0.00825	150 × 150	Yes	1:−0.39:−0.39
			(*c*) Series III			
PC7	Type I	0.0165	0.00825	—	—	1:0.32:0.32
PC8	Type II	0.0165	0.00825	150 × 150	No	1:0.32:0.32
PC9	Type III	0.0165	0.00825	150 × 150	Yes	1:0.32:0.32

Note: See Fig. 2 for details of panel type and of added reinforcement around opening.

inforcement consisted of 5.72-mm diameter deformed bar placed in two layers and oriented parallel to the sides of the panel. The reinforcing bars were typically spaced at 44.5 mm centers in the longitudinal direction and 89-mm centers in the transverse direction (see Fig. 2), resulting in nominal reinforcement ratios of $\rho_x = 1.65\%$ and $\rho_y = 0.82\%$, respectively. Further, short anchorage bars were provided at the edges, in the transverse direction, to ensure adequate load transfer. The clear cover provided to the outside reinforcement was 6 mm.

The details of the three types of panels tested are shown in Fig. 2. The type I panel in each series was a solid panel with a homogeneous grid of reinforcement. The type II panels contained a 150-mm square perforation at the center, with sides parallel to the sides of the panel. The reinforcement bars interrupted by the opening were hooked back, and no provisions were made for replacing the reinforcement lost. In the type III specimens, compensation was made for the interrupted reinforcement by providing reinforcement of equal cross-sectional area placed around the sides of the opening (see Fig. 2). The replacement bars extended an additional 150 mm beyond the opening, at each end, so as to provide sufficient development length. A 20-mm minimum cover was provided to the reinforcement at the sides of the opening.

Normal-density concrete was used in casting the panel specimens. The mix components were such as to provide a nominal strength of 25 MPa at seven days, using rounded aggregate of 10-mm maximum size. Standard tests performed on 150 by 300-mm cylinders yielded the concrete material properties summarized in Table 2. Note that the tensile strengths shown were determined from split-cylinder tests. A typical stress-strain curve for the concrete, determined on a stiff servo-controlled testing machine using a strain rate of 0.22×10^{-3}/sec, is shown in Fig. 3(a).

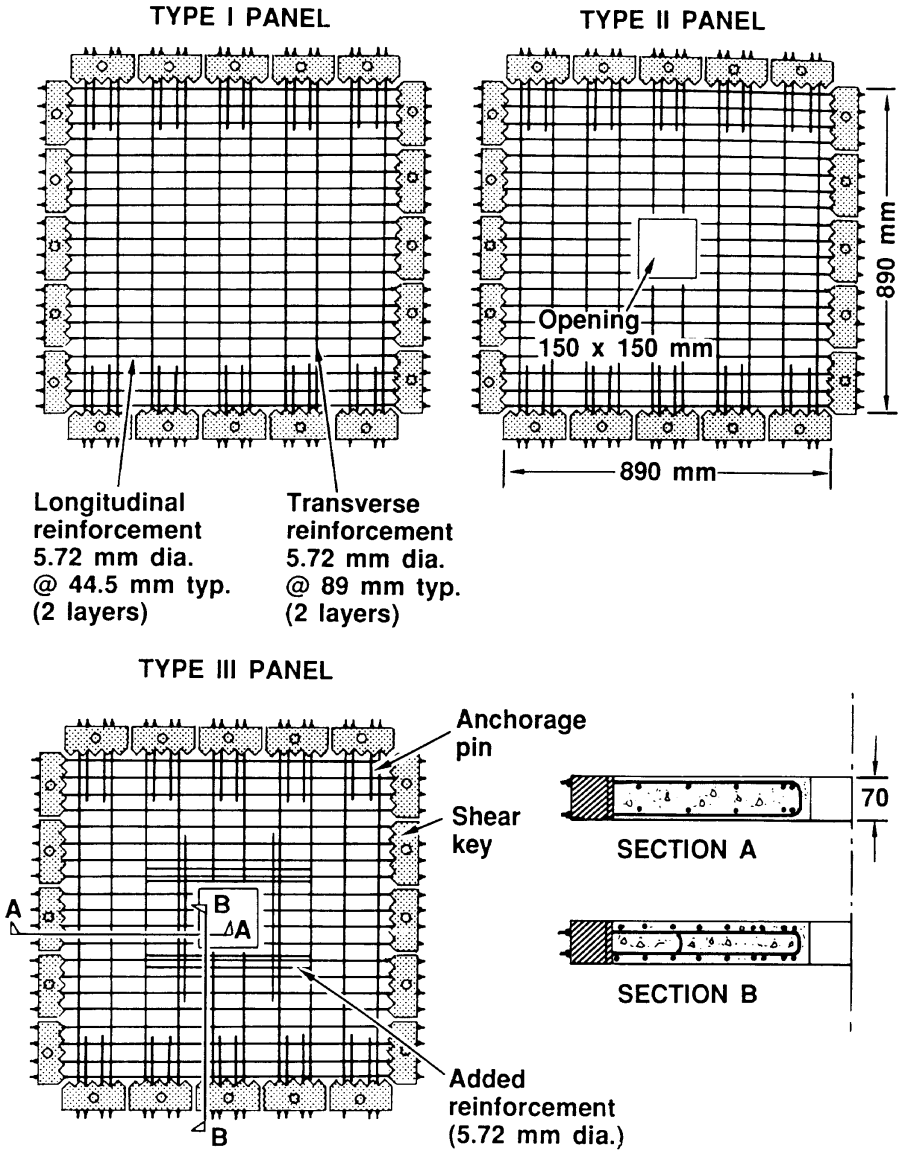

FIG. 2. Test Specimen Details

The reinforcing bars used in each of the three series of panels all came from the same stock. However, the reinforcing steel initially showed non-ductile behavior, with a 0.2% offset yield stress of 590 MPa and no yield plateau. Thus, the steel was subjected to heat treatment using commercially available facilities. The supply of bars was divided into three lots, one for each series of panels, and each lot was heat-treated separately but under similar specified conditions. The resulting reinforcing steel properties varied significantly between the three lots, but were reasonably uniform among the bars within any one lot. The reinforcement material properties determined are summarized in Table 2. Typical stress-strain response curves are shown in Fig. 3(*b*).

For load application purposes, five shear keys per side were cast integral with the panels. The reinforcing bars, machined to have threaded ends, passed through the shear keys and were fastened into place with nuts. The shear keys, in turn, fitted into the shear rig testing facility [see Fig. 4(*a*)]. This

TABLE 2. Material Properties

Panel number (1)	Concrete			Reinforcement		
	f'_c (MPa) (2)	f_{cr} (MPa) (3)	ϵ_0 ($\times 10^{-3}$) (4)	f_{ys} (MPa) (5)	f_u (MPa) (6)	E_s (MPa) (7)
PC1	25.1	2.45	1.83	500	570	196,800
PC1A	27.9	2.66	1.85	500	570	196,800
PC2	25.5	2.46	1.98	500	570	196,800
PC3	26.8	2.55	1.84	500	570	196,800
PC4	24.9	2.49	1.70	260	380	202,700
PC5	29.0	2.53	1.85	260	380	202,700
PC6	25.7	2.55	1.70	260	380	202,700
PC7	28.7	2.39	1.85	390	480	195,000
PC8	27.3	2.57	1.80	390	480	195,000
PC9	28.0	2.36	1.85	390	480	195,000

facility, described elsewhere (Vecchio and Collins 1986), allows panels to be loaded with any proportional or nonproportional combination of membrane shear and biaxial normal forces. The system of load application results in essentially uniform applied stresses along the panel edges.

Loads were applied to the test panels in a proportional and monotonic manner, up to failure. In the series I tests, the loading condition was pure shear ($v:f_x:f_y = 1:0:0$). For the series II tests, a condition of proportional biaxial compression and shear was applied in the ratio of $v:f_x:f_y = 1:-0.39:-0.39$. The series III tests involved the condition of shear and biaxial tension in the proportion of $v:f_x:f_y = 1:0.32:0.32$.

In a typical test, the course of loading was broken into stages. At each load stage, loading was suspended and the panel deformations were held constant as measurements and inspections were made and photographs were taken. Some relaxation in load occurred in the 20–30 min required for readings. Loading then resumed. Each test consisted of about 10 load stages, thus requiring about five hours to complete.

Surface strains were measured on both sides of a test panel using specially developed mechanical strain gages with electronic feed-outs, known as Zurich gages. Zurich readings were taken in the longitudinal, transverse, and two diagonal directions at each load stage, using a 200-mm gage length grid system encompassing the central 600-mm square area of the panel [see Fig. 4(*b*)]. Thus, a total of 42 Zurich strain measurements were made on each side of the panel. Displacement transducers (LVDTs) mounted onto the sides of the panel provided a continuous monitoring of average strain conditions. Electrical resistance strain gages, of 5-mm gage length, were applied to the reinforcement at various locations around the opening [see Fig. 4(*b*)]. These gave indications of local rebar stresses.

Pressure transducers, connected within the hydraulic system of the load facility, were used to determine the loads applied to the panel. Load cells, installed onto 13 of the 40 hydraulic cylinders used to apply load, provided an independent measure of the magnitude and uniformity of the loads ap-

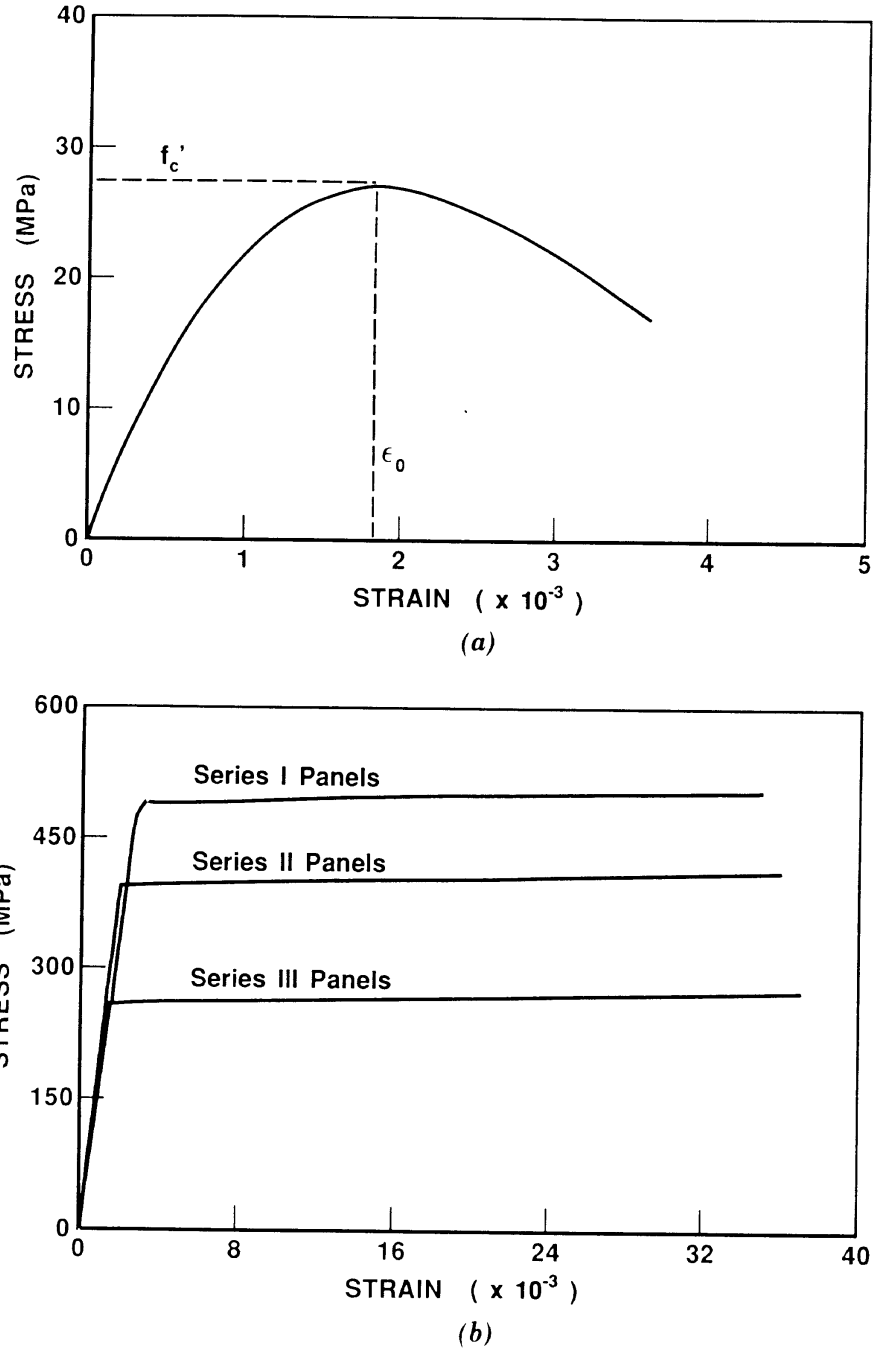

FIG. 3. Material Stress-Strain Behavior: (*a*) Concrete; (*b*) Reinforcement

plied. All instrument readings were continuously monitored and stored using a computer-controlled data acquisition system.

Test Observations

It was observed that the cracking, load-deformation response, ultimate strength, and failure mode of the panels were all significantly affected by the presence of an opening and by reinforcement detailing. This was equally apparent under all three loading conditions considered. Table 3 briefly summarizes the key results, including cracking load, ultimate load, and load at first yielding of the longitudinal and transverse reinforcement. Typical crack

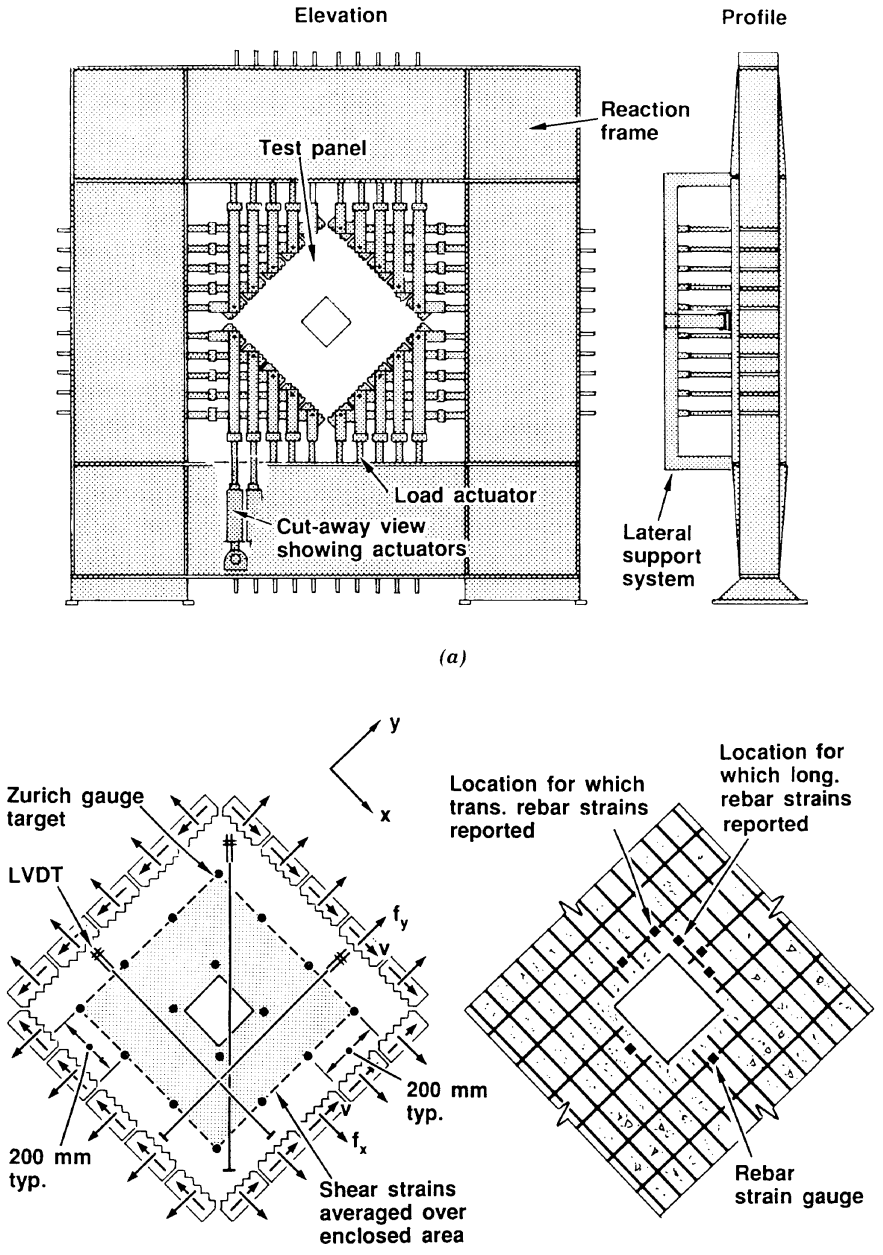

FIG. 4. Test Setup, Loading, and Instrumentation: (*a*) Shear Rig Test Facility; (*b*) Panel Loading and Instrumentation

and failure conditions observed are shown in Fig. 5. Fig. 6 shows the observed load-deformation responses of the panels as measured normal shear strain (i.e., relative to panel x, y axes) versus the applied shear stress. The shear strains shown were determined from the Zurich strain measurements averaged over the central 600-mm square area of the panel. The shear stresses plotted are the nominal values determined from the loads applied on the panel edges.

The type I panels (i.e. solid panels: PC1, PC4, and PC7) generally exhibited a linear response up to the cracking load, the level of which depended greatly on the loading condition (see Table 3). Beyond cracking, a gradually softening load-deformation response was observed, reflecting the influence

TABLE 3. Summary of Test Results

Panel number (1)	v_{cr} (MPa) (2)	v_{yy} (MPa) (3)	v_{yx} (MPa) (4)	v_u (MPa) (5)	Failure mode (6)
PC1	1.96	—	—	4.95	Premature edge failure
PC1A	2.17	5.29	—	5.61	Concrete shear/crushing
PC2	1.74	4.10	—	4.37	Concrete shear/crushing
PC3	1.90	4.83	—	4.83	Concrete shear/crushing
PC4	3.00	4.75	—	4.84	Concrete shear/crushing
PC5	2.32	3.84	—	3.84	Concrete shear/crushing
PC6	2.50	3.97	—	4.35	Concrete shear/crushing
PC7	1.50	3.34	—	3.65	Edge failure
PC8	1.10	2.41	2.79	2.79	Concrete shear/crushing
PC9	1.35	2.86	3.01	3.09	Concrete shear/crushing

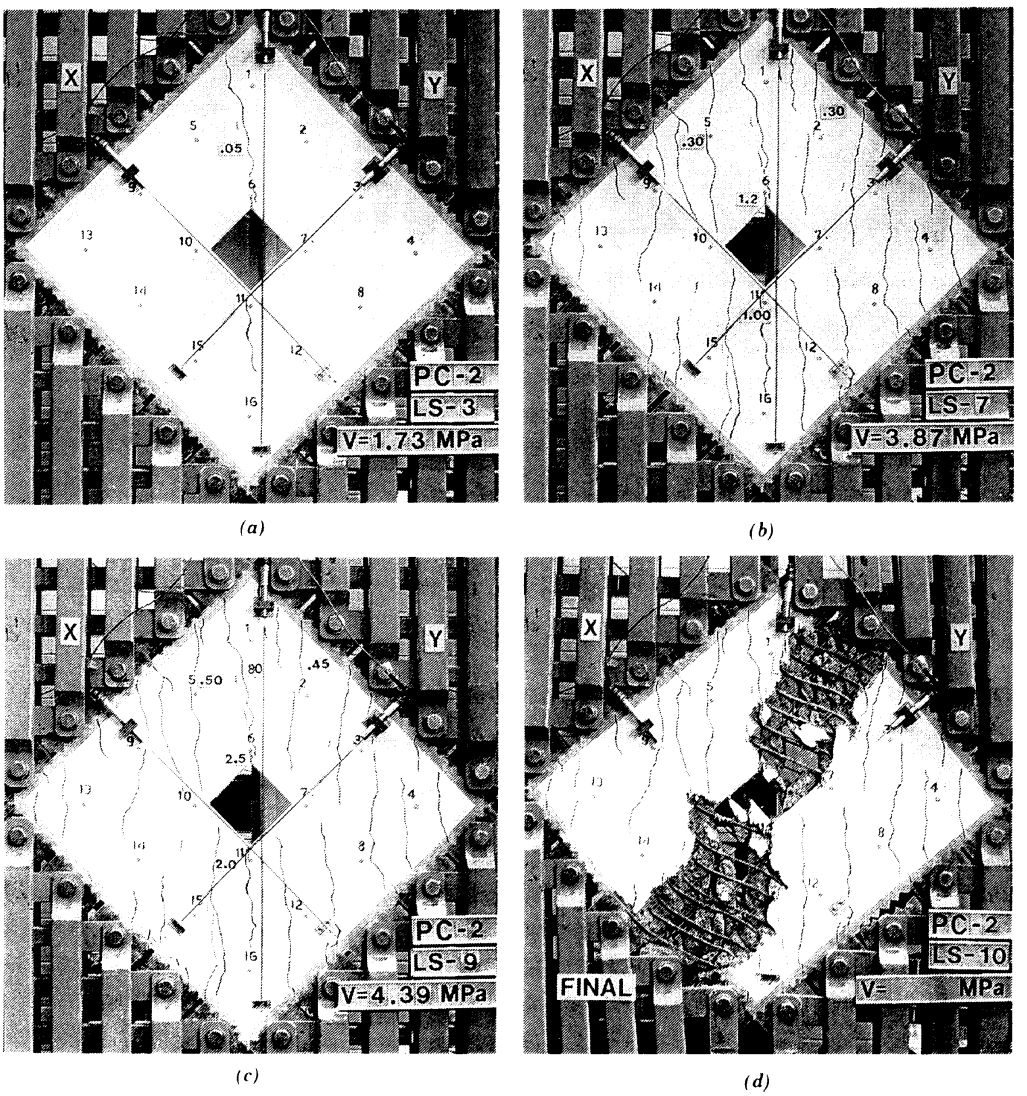

FIG. 5. Photographs of Panel PC2 during Testing: (*a*) Initial Cracking; (*b*) Rebar Yielding at Opening; (*c*) Just Prior to Failure; (*d*) Shear/Crushing Failure

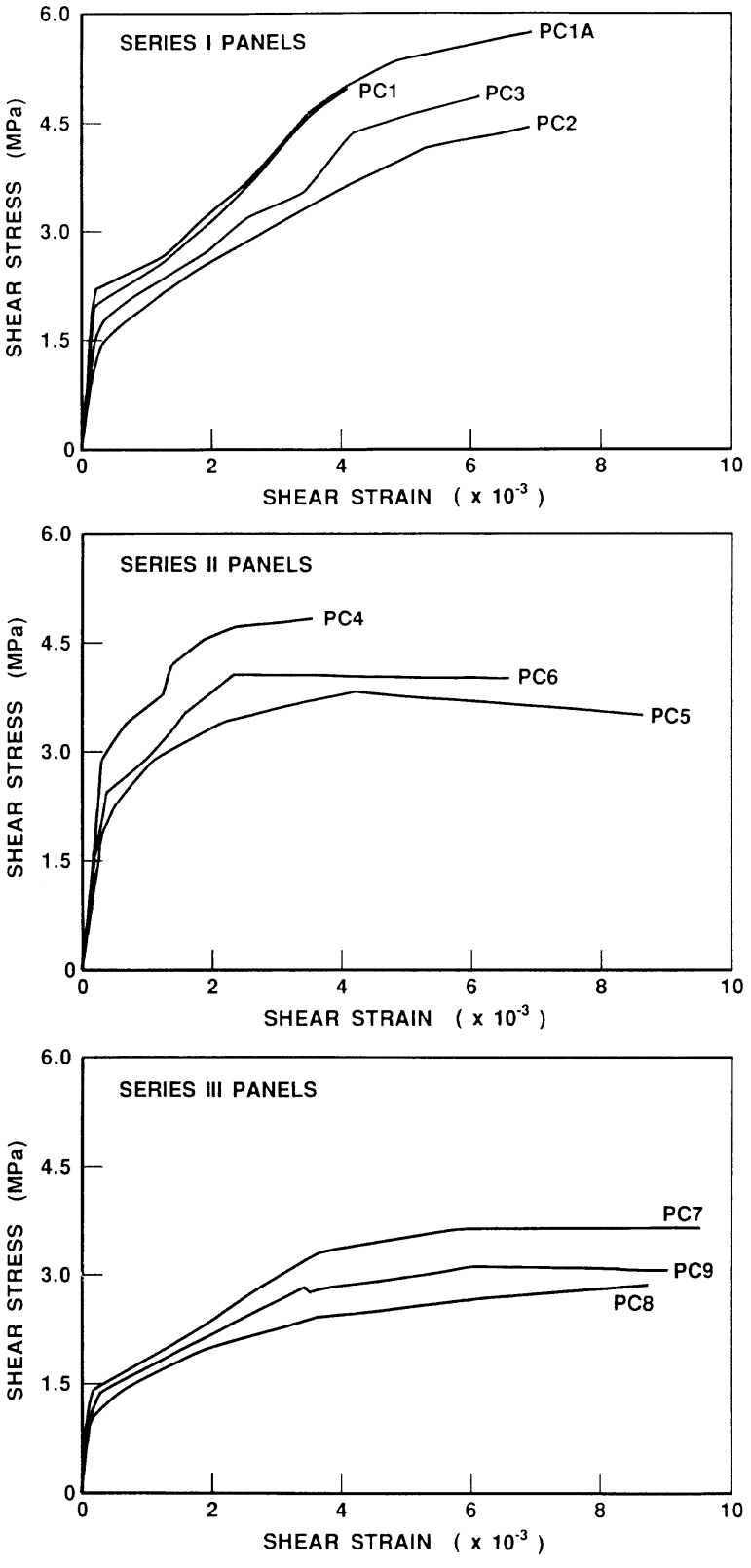

FIG. 6. Observed Load-Deformation Response of Test Panels

of concrete tension-stiffening mechanisms (see Fig. 6). Cracking and strain conditions developed uniformly over the entire area of the test panels. At advanced stages of loading, the reinforcement in the transverse direction yielded. Shortly after, a ductile failure of the panel occurred, involving a crushing/shear failure of the concrete. The longitudinal reinforcement did not yield.

With the type II panels (i.e., panels with opening but no added reinforcement: PC2, PC5, and PC8), first cracking was detected at loads much lower than those observed in the corresponding solid panels. Cracking typically initiated at the top and bottom corners of the opening (see Fig. 5). Increases in load thereafter caused cracking to gradually propagate over the entire panel area. Distress was generally most apparent around the opening, as severe cracking, yielding of reinforcement, and crushing of concrete were localized in these regions. The resulting load-deformation responses of the panels were considerably less stiff than those observed in the corresponding solid panels (see Fig. 6). At ultimate, a ductile shear failure developed after yielding of the reinforcement in the transverse direction. In panel PC8, local yielding of the longitudinal reinforcement near the opening was also experienced. The ultimate load capacities of the type II panels were considerably reduced compared to those of the corresponding type I panels.

The type III panels (i.e. panels with opening and added reinforcement: PC3, PC6, and PC9) demonstrated a behavior intermediate to that of the corresponding type I and type II panels. First cracking was again initiated at the corners of the perforation but at slightly higher loads than in corresponding panels without added reinforcement (see Table 3). As the loads increased, visible distress zones were limited to small regions in the vicinity of the opening, and crack widths were significantly less compared to those in the corresponding type II panels. The post-cracking load-deformation response was also seen to be significantly stiffened with the addition of reinforcement around the opening but remained lower than that obtained with the solid panels (see Fig. 6). Further, the ultimate load capacity attained was intermediate to those of the other panels in the same series. The failure mode at ultimate involved a crushing shear failure of the concrete occurring soon after yielding of the transverse reinforcement and was generally more brittle and sudden. In panel PC9, localized yielding of the longitudinal reinforcement was also observed.

Stresses in the reinforcement, as determined from strain gages, were also seen to be highly influenced by the presence of an opening. Shown in Fig. 7 are the strains measured in the longitudinal and transverse reinforcement at locations near the opening (see Fig. 4 for gage locations). For the solid panel specimens, the strains shown are the values averaged over the entire specimen area. It can be seen that in all cases, the stress disturbances created by the openings resulted in a significant increase in local rebar strains as compared to the solid panels. The effect was particularly prevalent in the type II panels, containing no added reinforcement around the opening.

The loading conditions imposed also resulted in perceptible differences in behavior. The series III specimens, tested in biaxial tension and shear, developed a pattern of closely spaced cracks (80–100-mm average spacing) and demonstrated high degrees of ductility. Conversely, the series II panels, tested in biaxial compression and shear, exhibited considerably less cracking (average spacing 125–150 mm) and less ductile behavior. The failure modes,

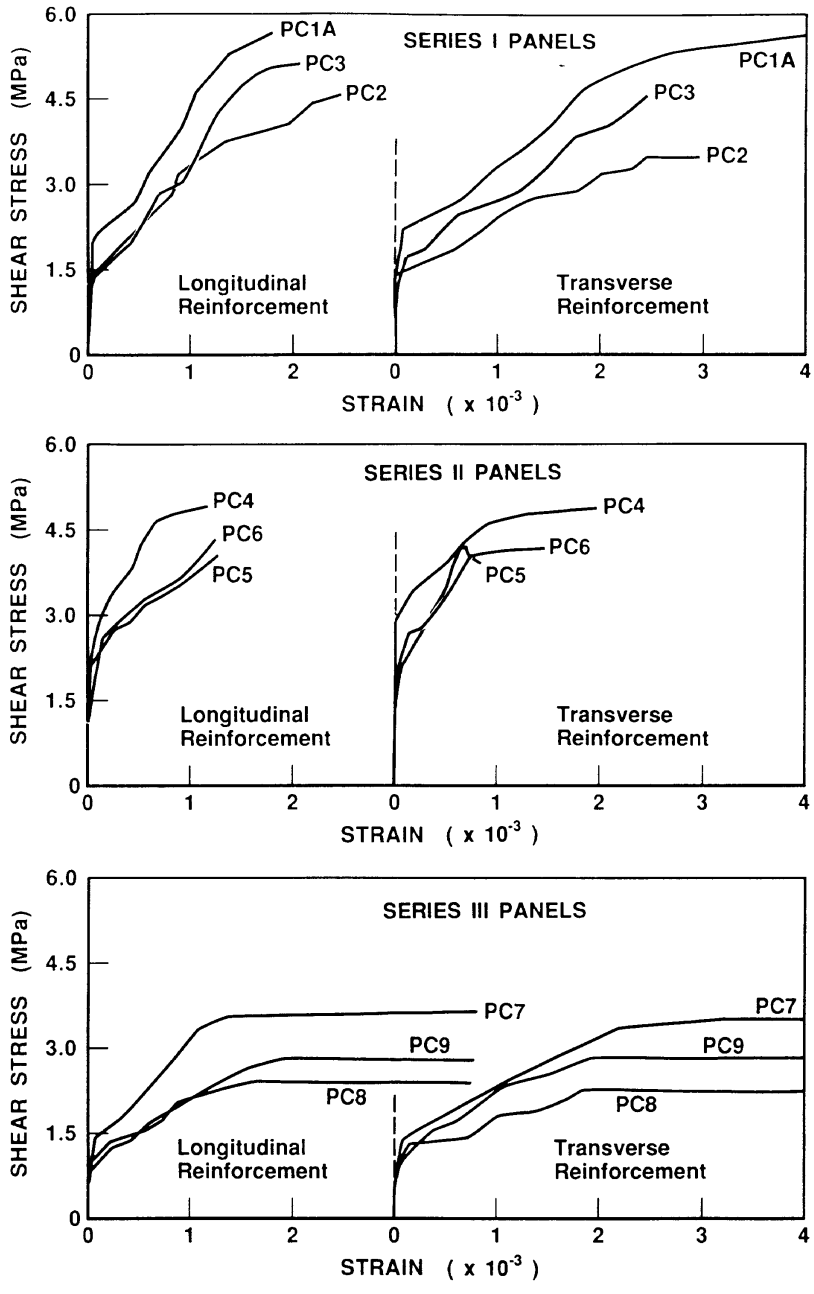

FIG. 7. Measured Rebar Strains in Test Panels

while involving a shear failure of the concrete in all cases, were generally more sudden and brittle with the series II panels.

ANALYSIS

The perforated type II panels effectively contained 20% less reinforcement in both the longitudinal and transverse directions, at sections taken through the opening, compared to the reinforcement amounts provided in the solid panels. Further, at these sections, the cross-sectional area of concrete was reduced by about 17%. In the type III panels, the reduction in concrete area was similar, but the reinforcement amounts were increased back to the levels provided in the solid panels. In consideration of these figures, it is interesting

to compare the reductions in ultimate load capacity observed in the test panels.

Averaged over the three series of tests, the type II panels demonstrated a 22% reduction in ultimate capacity (i.e., v_u), and the type III panels exhibited a 13% reduction (see Table 3). Thus, for the panels without added reinforcement around the opening, the reduction in ultimate strength was slightly in excess of the reduction in reinforcement provided. This would suggest that the influence of the opening in disturbing the uniformity of stresses within the panels actually resulted in only a marginal decrease in strength per unit area. Consider, however, the strength reductions observed in the type III panels, in which the total reinforcement amounts were similar to those provided in the solid panels. Here, it is important to recognize that although yielding of the reinforcement preceded failure, and although the principal compressive stresses in the concrete were considerably less than the concrete cylinder strengths, final failure of the panels involved a failure of the concrete. Thus, strain-softening of the concrete in compression, coupled with the stress disturbances caused by the opening, had a significant influence on strength. Note, too, that the strength reductions were essentially of the same proportion under all three loading conditions.

The influence of the load conditions on the ultimate strengths can also be examined to some extent, although the significantly different steel yield strengths among the three series of panels make a direct comparison difficult. Generally, the smaller magnitude of strains encountered under conditions of compression and shear allowed higher concrete crushing strengths, and thus higher panel shear strengths, to be attained. Under conditions of tension and shear, the generally larger strains resulted in more pronounced strain-softening effects, and thus lower strengths.

It is also significant to note that a high degree of ductility in response of the panels was preserved in all cases, regardless of the disturbing influence of the openings. Further, the final failure mode was unchanged from one involving a shear failure of the concrete. However, this will not always be the case. In panels that are lightly reinforced in one or both directions, the effects of an opening may result in a change in failure mode from ductile yielding of the reinforcement to concrete shearing. In very heavily reinforced panels, a more brittle concrete crushing failure may be triggered by the stress concentrations created around an opening. In either case, the ductile nature of the load-deformation response may also be adversely affected.

Theoretical Response

Theoretical predictions of the panels' response were obtained from finite element analyses. The analysis program used, known as TRIX and described in Vecchio (1990), employs a nonlinear analysis algorithm based on a secant stiffness formulation. Incorporated into the program formulation are constitutive models for concrete and reinforcement based on the modified compression field theory (Vecchio and Collins 1986). Thus, the analyses inherently accounted for the effects of strain softening of the concrete in compression and the influence of post-cracking tensile stresses in concrete.

The finite element mesh used to represent the perforated panels is shown in Fig. 8(*a*). The panel reinforcement was modeled using a smeared approach, defined for each element in terms of reinforcement ratios. For the type II panels, all elements in the mesh were specified as having the rein-

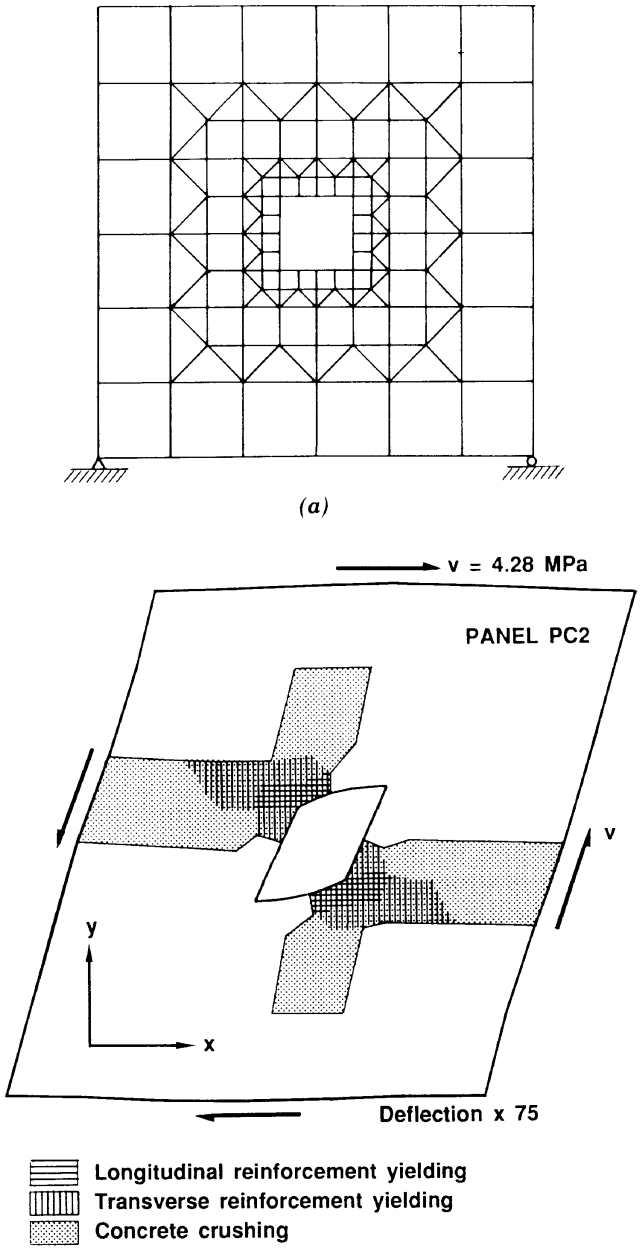

FIG. 8. Finite Element Modeling of Test Panels: (*a*) Finite Element Mesh; (*b*) Conditions in Panel PC2 at Ultimate Load

forcement ratios $\rho_x = 0.165$ and $\rho_y = 0.00825$. For the type III panels, the reinforcement ratios for the elements within a 75-mm wide band around the opening were increased in accordance to the additional reinforcement provided. For the solid type I panels, a single-element model was used with $\rho_x = 0.0165$ and $\rho_y = 0.00825$. In all cases, the material properties used for the concrete and reinforcement were as specified in Table 2.

The complete load-deformation response of each panel was computed under loads corresponding to test conditions. Comparisons of the experimentally observed behavior with the theoretically predicted responses are shown in Fig. 9. Generally, good agreement is seen in most aspects of behavior, including precracking stiffness, cracking load, post-cracking deformations,

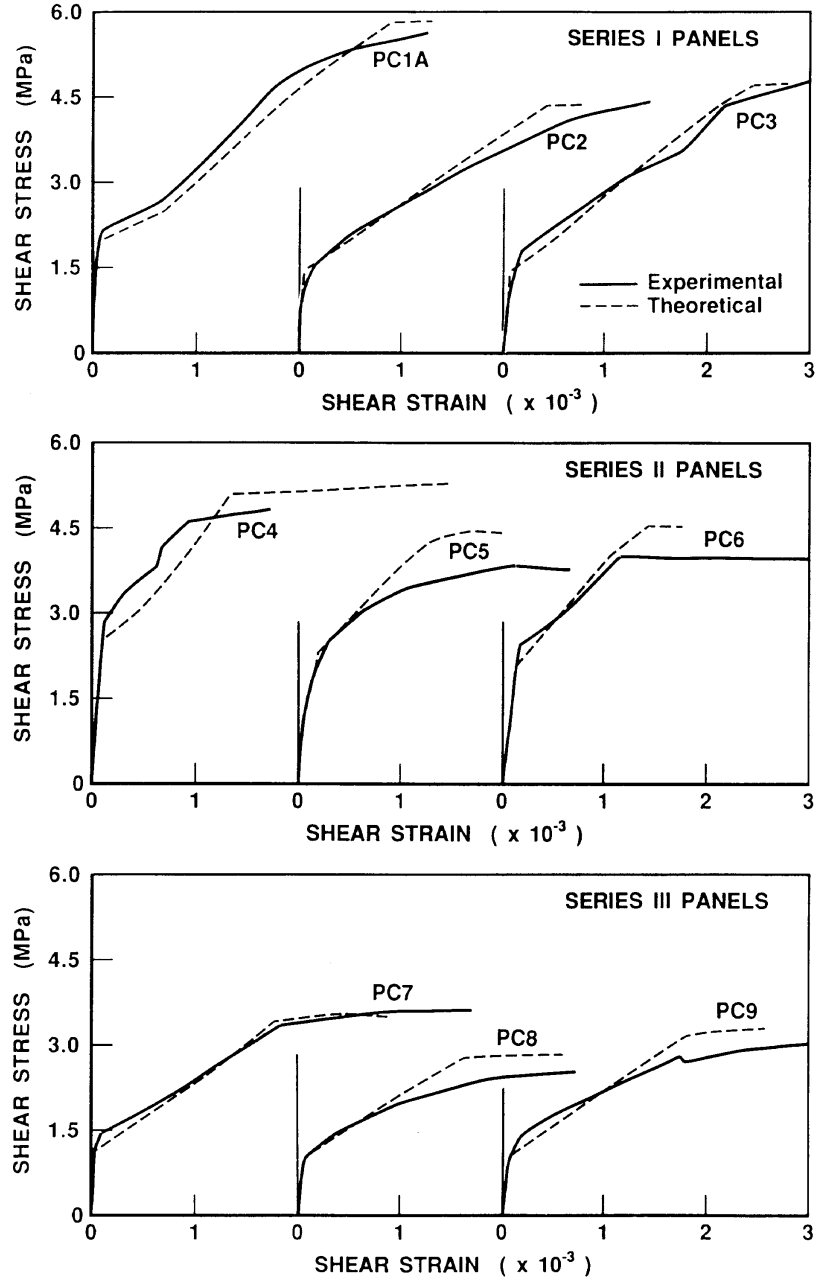

FIG. 9. Comparison of Theoretical and Experimental Load-Deformation Response

and ultimate load capacity. Particularly significant is the ability to predict a gradually softening post-cracking response for the type I panels. Also predicted well, in general, were the location and orientation of cracks and the loads at which they occurred. Post-ultimate behavior (i.e., ductility), however, was not modeled well because of the load-control nature of the finite element program formulation. Further, the stiffness of the panels subjected to combined biaxial compression and shear appears to be overestimated.

The ultimate load capacities and failure modes of the panels were captured well in the theoretical analyses. For the nine panels tested, the ratio of the experimental to theoretical strength ($v_{u_{exp}}/v_{u_{theor}}$) had a mean value of 0.97 and a coefficient of variation of 5.6%. The predicted mode of failure at ultimate

load, for all panels, involved a shear failure of the concrete along a plane passing through the corners of the perforation. This corresponds well to the observed mechanism of failure. Shown in Fig. 8(*b*) are the predicted conditions in panel PC2 just prior to failure. It can be seen that the predicted areas of distress correspond reasonably well to what can be seen in Fig. 5 as the actual eventual failure.

The ability to predict straining in the reinforcement was also examined. Shown in Fig. 10 are the strains in the longitudinal and transverse reinforcement of the series I panels, at locations near the opening (see Fig. 4 for locations). The theoretical predictions appear to model reasonably well the measured values, with a slight tendency to overestimate. Similar agreement

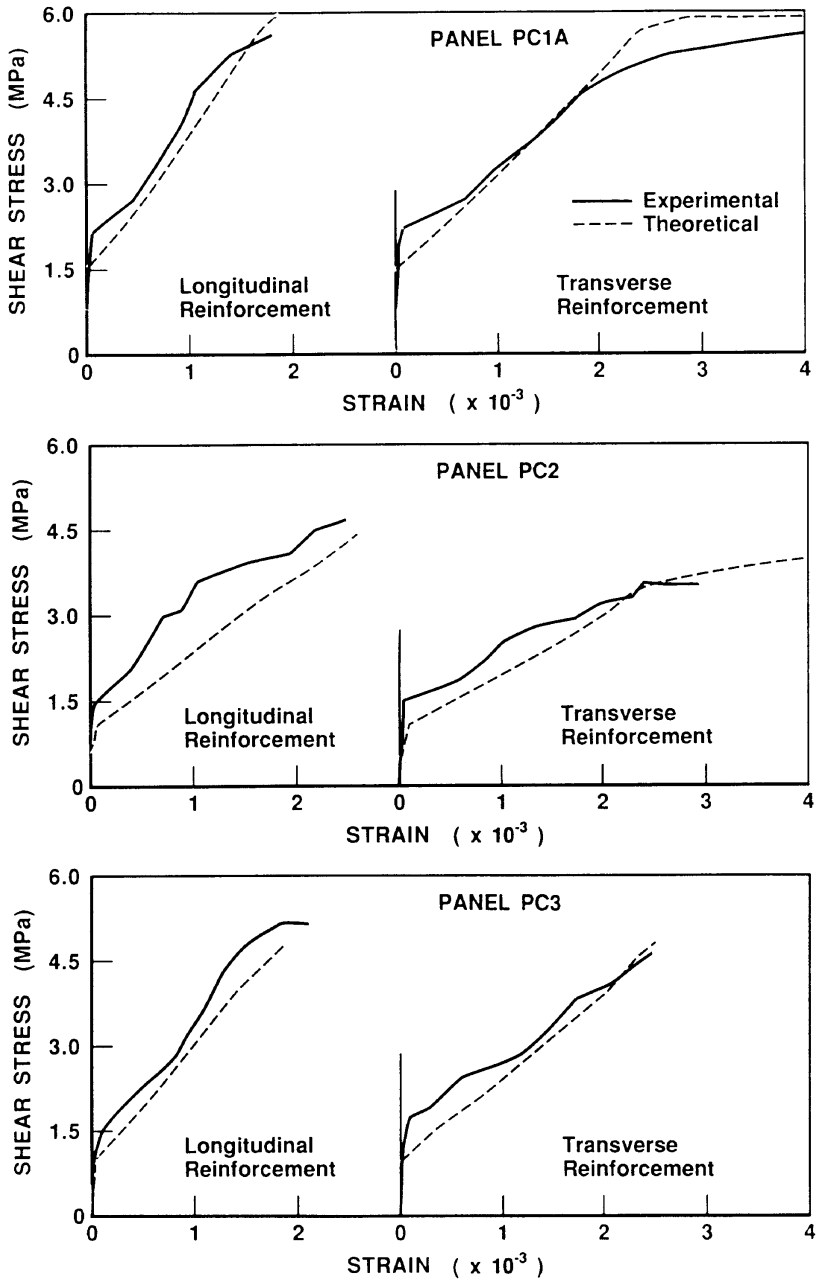

FIG. 10. Comparison of Theoretical and Experimental Rebar Strains for Series I Panels

was obtained for the other panels. It should be noted, however, that both the experimental and theoretical values are highly sensitive to location and to concrete cracking.

It is anticipated that more accurate predictions of strength and deformation response could be obtained if a finer element mesh were used to represent the test panels. The relatively coarse mesh used was necessitated by the memory limitations of the personal computer on which the analysis program was developed. Advanced versions of the program, for use on more powerful systems, are now being developed.

Conclusions

A test program was undertaken in which reinforced concrete panel elements containing perforations were subjected to in-plane load conditions. The specimen parameters included presence of a center perforation, detailing of reinforcement around the opening, and type of loading condition.

The test program was successful in providing data relating to the behavior of reinforced concrete elements under simple and well-defined conditions, but where internal discontinuities had a significant effect on overall element response. This data set will serve as a useful addition to those currently available in the literature for calibrating or verifying analytical procedures.

The test results indicated that the detrimental effects of a perforation are typically greater than can be directly attributable to reductions in areas of concrete or reinforcement. Localized cracking, yielding of reinforcement, or crushing of concrete around the opening can lead to a significant reduction in the overall strength and stiffness of the element. Added reinforcement around the opening can be effective to a partial extent in alleviating the detrimental effects.

A nonlinear finite element procedure, based on the modified compression field theory, was used to predict the response of the test panels. It was found that this formulation provided reasonably accurate predictions of both ultimate strength and load-deformation response. Thus, the ability of the modified compression field theory to accurately model behavior in situations involving complex local stress conditions was demonstated. Also reaffirmed was the understanding that a proper consideration of concrete compression strain-softening effects and tension-stiffening effects is essential to obtaining accurate predictions of behavior.

Acknowledgments

The work presented in this paper was made possible through funding from the Natural Sciences and Engineering Research Council of Canada. The writers wish to express their sincere gratitude for the support received.

Appendix I. References

ACI Committee 313. (1983). "Recommended practice for design and construction of concrete bins, silos, and bunkers for storage of granular materials." *ACI 313-77*, American Concrete Institute, Detroit, Mich.

Haydl, H. M. (1987). "Analysis of a large cut-out in a circular silo wall." *ACI Struct. J.*, 84(3), 262–265.

Mansur, M. A., Tan, K. H., and Lee, S. L. (1985). "Design method for reinforced concrete beams with large openings." *ACI J.*, 82(4), 517–524.
Pool, R. B., and Lopes, R. (1986). "Cyclically loaded concrete beams with web openings." *ACI J.*, 83(5), 757–763.
Sato, Y., et al. (1987). "Load-deflection characteristics of shear walls with openings." *Proc., Ninth Int. Conf. on Structural Mechanics in Reactor Technology, Lausanne 1987*, Vol. H, 537–542.
Vecchio, F. J. (1989). "Nonlinear finite element analysis of reinforced concrete membranes." *ACI Struct. J.*, 86(1), 26–35.
Vecchio, F. J. (1990). "Reinforced concrete membrane element formulations." *J. Struct. Engrg.*, ASCE, 116(3), 730–750.
Vecchio, F. J., and Collins, M. P. (1986). "The modified compression field theory for reinforced concrete elements subjected to shear." *ACI J.*, 83(2), 219–231.

APPENDIX II. NOTATION

The following symbols are used in this paper:

E_s = modulus of elasticity of reinforcement;
f_{cr} = concrete cracking stress;
f_x = normal stress applied on panel edges, x-direction;
f_y = normal stress applied on panel edges, y-direction;
f_{ys} = reinforcement yield stress;
f'_c = compressive strength of concrete cylinder;
v = shear stress applied on panel edges;
v_{cr} = shear stress at first cracking;
v_u = ultimate shear stress capacity;
v_{yx} = shear stress at first yielding of longitudinal reinforcement;
v_{yy} = shear stress at first yielding of transverse reinforcement;
ϵ_0 = strain in concrete cylinder at peak stress f'_c;
ρ_x = steel reinforcement ratio in longitudinal direction; and
ρ_y = steel reinforcement ration in transverse direction.